Scientific paper

Influence of Surface Energy on Compressive Strength of Concrete under Static and Dynamic Loading

Hiromichi Matsushita[1] and Kouzou Onoue[2]

Received 27 March 2006, accepted 14 June 2006

Abstract

To clarify the compressive static and fatigue strength of concrete immersed in various liquids, experimental studies were conducted. The influence of the surface tension of immersion liquid on static and fatigue strength of concrete were examined based on the knowledge that (1) the fracture process of concrete at the macro scale is the result of generation and propagation of internal microcracks, (2) strain energy is partially released as surface energy when microcracks are formed, and (3) the magnitude of the surface energy between a solid and a liquid is affected by the surface tension of the liquid. The results indicate that the larger the surface tension of the immersion liquid, the smaller the static and fatigue strength of concrete, and that these are characterized by a linear relationship. It also became clear that the fatigue of concrete in air hardly matters whereas special attention should be given to the fatigue of concrete in the case of concrete structures that are frequently immersed in liquid with a larger surface tension than water, such as marine structures.

1. Introduction

It is socially required that both newly built and existing concrete structures be managed properly and utilized effectively. For that purpose, the state of concrete should be estimated correctly for the accurate prediction of its durability.

The compressive strength of concrete is one of the basic engineering indicators in the design of concrete structures. However, the compressive strength of concrete fluctuates significantly depending on the moisture content. It is well known that the compressive strength of concrete in water is 10% to 20% smaller than that in air. This fact is important for the design of any concrete structure, but in practice the influence of moisture on the compressive strength of concrete is not usually taken into account.

There have been various discussions about the reason for the moisture dependency of the compressive strength of concrete. Representative examples of the mechanism are as follows: (1) pore water pressure helps separation at the tip of the microcracks because incompressible water gets wedged into the cracks (Pickett 1956; Troxell 1958; Oshita and Taniguchi 1999), and (2) the surface energy that forms new microcracks decreases because moisture adheres to the surface of microcracks (Hori 1962; Okajima and Ishikawa 1981; Wittmann 1983; Ogishi *et al.* 1986; Asamoto and Ishida 2004; Cook and Haque 1974). However, no consensus has yet been reached. To account properly for the influence of moisture content on the compressive strength of concrete, the mechanism that is involved has to be clarified.

2. Fracture process of concrete under uniaxial compression

Basically, the fracture process of concrete at the macro scale is the generation and propagation of internal microcracks. When concrete is loaded, strain energy is stored in the concrete. The greater the loading, the greater the strain energy. When the value of the strain energy reaches the limit, a part of the strain energy is released in the form of microcracks. Most of the strain energy is released as surface energy, and the remainder is consumed as light, heat, sound or magnetism. According to Griffith (1920), when the value of the released strain energy becomes equal to the surface energy on the new microcracks, the microcracks stop growing. However, further increases in loading result in further accumulation of strain energy. When the value of the strain energy reaches the limit again, microcracks are formed again and a part of the strain energy is released as surface energy and other types of energy. Through a repetition of these processes, the microcracks start interconnecting and the damage in the concrete progresses at an accelerated pace. Thus, the strength of concrete is highly related to microcracks, and surface energy is indispensable to the formation of microcracks.

On the other hand, according to Young's equation, solid-liquid interface energy is equal to the difference between solid and liquid surface energies as given by Eq.1.

$$\gamma_{sl} = \gamma_s - \gamma_l \cos\theta \qquad (1)$$

where,

γ_{sl}: solid-liquid interface energy
γ_s: solid surface energy

[1]Professor, Faculty of Engineering, Kyushu University, Japan.
E-mail:matsu@doc.kyushu-u.ac.jp
[2]Research Associate, Faculty of Engineering, Fukuoka University, Japan.

γ_l: liquid surface energy
θ: contact angle between liquid and solid

If moisture adheres to the surface of microcracks, the liquid surface energy, γ_l, increases and the solid-liquid interface energy, γ_{sl}, decreases. In that case, the strain energy that should be released on new microcracks becomes redundant, and the microcracks grow further. In general, the contact angle between water and cement based materials is said to be equal to zero because of the high hydrophilic property of cement gel particles (Asamoto and Ishida 2004), so the value of $\cos\theta$ can be considered equal to 1.

Griffith's theory deals with a situation in which tensile force works on an ideal crack. On the other hand, it is thought that the fracture process of concrete under uniaxial compression is the generation and propagation of many microcracks and that several fracture modes are mixed. Thus, the theory cannot be applied directly to the compressive fracture process of concrete. However, even if concrete is under compression, surface energy is indispensable for the formation of microcracks, and it is highly predictable that the compressive strength of concrete depends on the surface energy.

Hori (1962) measured the bending strength of mortar specimens submerged in various kinds of liquids with different surface tensions. **Figure 1** shows the relationship between the surface tension of immersion liquid and the bending strength of mortar. The bending strength of mortar decreases linearly with increases in the surface tension of immersion liquid.

As studies on compressive strength of cement based materials from the viewpoint of surface energy, the works of Okajima and Ishikawa (1981), Ogishi *et al.* (1986), Asamoto and Ishida (2004) and Cook and Haque (1974) can be listed. These studies conclude that the reason for the lowering of the compressive strength of concrete in a wet condition is due to the decrease in surface energy. However, in these studies the number of liquids with different surface tensions is limited. Moreover, there have been no detailed studies on the relationship between the surface tension of immersion liquid and the compressive strength of concrete. Therefore, more data needs to be obtained for a systematic knowledge of how liquid affects the lowering of the strength of concrete when the water-cement ratio or other conditions are changed.

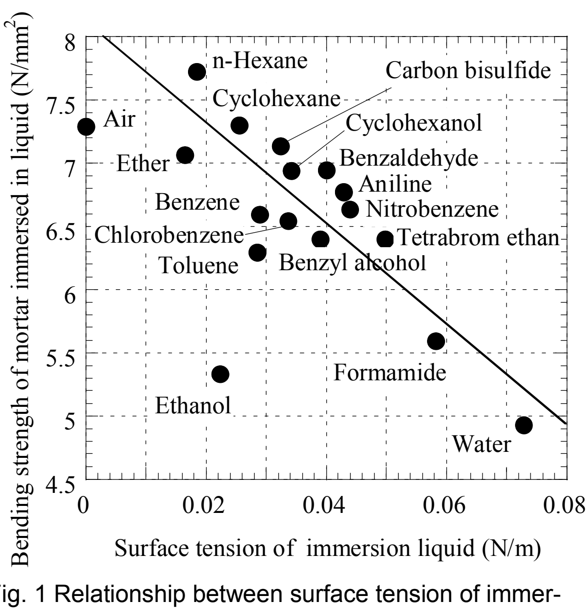

Fig. 1 Relationship between surface tension of immersion liquid and bending strength of mortar (Hori 1962).

3. Influence of surface tension of immersion liquid on compressive strength of mortar

3.1 Methods and materials

The mortar mixture used in the experiment is shown in **Table 1**. Ordinary Portland cement (specific gravity = 3.16, specific surface = 0.327 m^2/g) and sea sand (specific gravity in saturated surface-dry condition = 2.57, water absorption = 1.60%) were used. Prism specimens (height = 40 mm, width = 40 mm, length = 160 mm) were used. Compressive strength tests were performed in accordance with JIS R 5201 (Physical testing methods for cement).

Figure 2 shows the setting of the compressive test. Compressive tests were conducted on mortar specimens submerged in non-corrosive organic solvents or water. The values of the surface tensions of all the different liquids used in this study are listed in **Table 2**. Mortar specimens were underwater cured for 28 days, then dried in a drying furnace at 110 degrees C untill the weights of specimens became constant. Then the specimens were submerged in liquid untill their weights became constant. When water was used as the immersion liquid, the compressive tests were performed immediately after the

Table 1 Mixture of mortar used in the experiment.

W/C (%)	S/C	Unit quantity (kg/m^3)		
		Water	Cement	Sand
50	2.4	284	567	1361

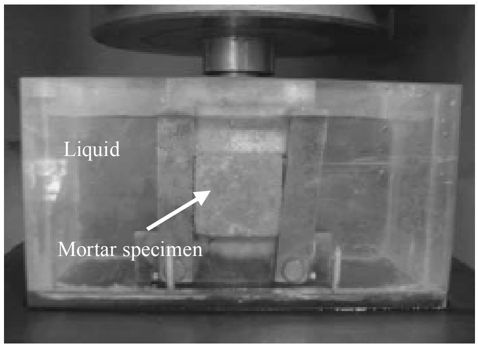

Fig. 2 Setting of compressive test.

Table 2 Surface tensions of immersion liquids.

Liquid	Surface tension (N/m)
Diethyl ether	0.0170
Hexane	0.0184
Ethanol	0.0227
Cyclohexane	0.0255
Phenylcarbinol	0.0390
Benzaldehyde	0.0400
Water	0.0728

underwater curing period. When no liquid was used, the compressive tests were performed after the specimens were dried completely in the drying furnace and cooled at room temperature.

3.2 Experimental results

Figure 3 shows the experimental result of compressive strengths of mortar in various kinds of liquids. The value of the compressive strength is the average of 6 data. The kind of liquid can be seen to affect the mean value and the standard deviation of compressive strength of mortar to a remarkable degree.

Figure 4 shows the relationship between the surface tension of the immersion liquid and the compressive strength of the mortar. The compressive strength of the mortar decreases linearly with increases in the surface tension of the immersion liquid. Griffith's equation tells us that we should not expect a linear relation between strength and surface tension, with strength depending instead on the square root of the surface tension. The authors plotted the strength data against the square root of the surface tension, revealing a linear relationship. No significant difference was confirmed. The same tendency for the bending strength has been reported by Hori (1962).

A regression line was obtained from seven data except for the ethanol plot. The reason why the compressive strength of mortar immersed in ethanol decreased significantly has not yet been elucidated. A same phenomenon for the bending strength has been reported by Hori (1962). Further studies are needed in this matter. However, in practice, the likelihood of concrete structures coming into contact with ethanol is low. Thus it is possible to state that the compressive strength of mortar decreases linearly with increases in the surface tension of the immersion liquid.

During compression testing, the temperature of the liquid adjacent to microcracks may rise due to the heat generated by friction between solid particles. In such a case, the surface tension of the immersion liquid decreases because the molecules are excited by the temperature rise. For example, the surface tension of water is 0.0746 N/m at 10 degrees C, 0.0723 N/m at 25 degrees C and 0.0700 N/m at 40 degrees C. In other words, the surface tension of water decreases 0.000153 N/m per 1 degree C of increase in temperature. Therefore, the surface tension of the liquid adhering to the surface of microcracks may be different from the values shown in **Table 2**. It is practically impossible to measure the local temperature change in concrete and the extent to which the surface tension of the immersion liquid changes is uncertain. Even if the surface tension of the liquid changes slightly due to a local temperature rise, it is possible to observe a large influence of the surface tension of the immersion liquid on the compressive strength.

On the other hand, according to Eq.1, solid-liquid interface energy is affected by the contact angle. As stated above, however, cement gel particles are highly hydrophilic and the contact angle between water and cement based materials is considered to be almost zero. Moreover, it is assumed that the surfaces of new microcracks are in high energy states, and on such surfaces almost all liquids will spread. Thus, the contact angles between

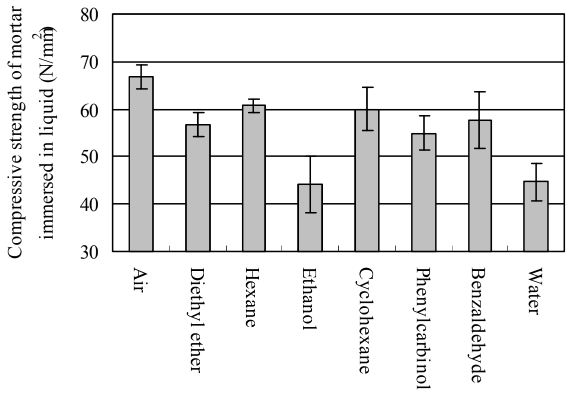

Fig. 3 Compressive strength of mortar saturated with various liquids.

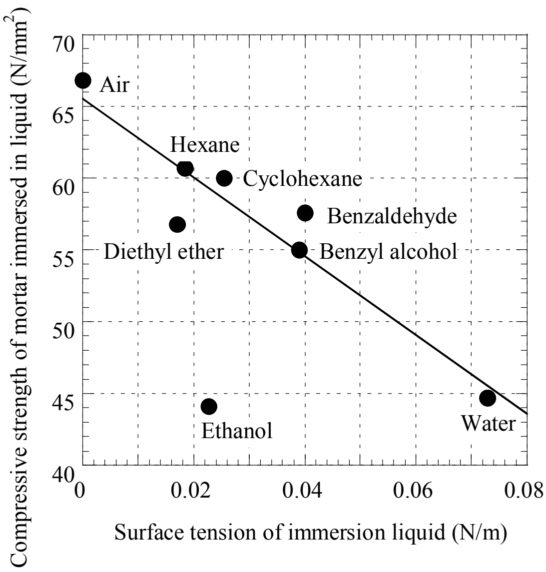

Fig. 4 Relationship between surface tension of immersion liquid and compressive strength of mortar.

other liquids than water and cement based materials are also considered to be almost zero. The solid-liquid interface energy that forms new microcracks was thus found to decrease linearly with increases in the surface tension of the immersion liquid, and the compressive strength of mortar to decrease.

The fact mentioned above is the result of the case in which the water-cement ratio of mortar was 50%. However, if the water-cement ratio of mortar is different, the surface energy of the solid will also differ, and further studies are needed to cover such cases. Furthermore, if the kind of cement based material is different, such as cement paste or concrete, the generation and propagation process of microcracks will also be different. The authors therefore selected several data on the relationship between compressive strength and the surface tension of the immersion liquid from the literature (Asamoto and Ishida 2004; Cook and Haque 1974) and compared them with the data obtained in this study.

The data cited from the literature on the compressive strengths of cement based materials submerged in various kinds of liquids with different surface tensions are summarized in **Table 3**. The values of compressive strengths differ considerably according to the type of cement based material, the water-cement ratio, and the immersion liquid.

To compare those data, compressive strength ratios were calculated and plotted against the surface tension of the immersion liquid. The compressive strength ratio is given by Eq.2.

$$\text{Compressive strength ratio} = f'_{c\text{-}l} / f'_{c\text{-}w} \tag{2}$$

where,

$f'_{c\text{-}l}$: compressive strength of cement based materials in liquid (N/mm^2)

$f'_{c\text{-}w}$: compressive strength of cement based materials in water (N/mm^2)

The results are shown in **Fig. 5**. There are linear relationships between the compressive strength ratios and the surface tensions of immersion liquids. The regression equation expressed by Eq.3 can be proposed.

$$\frac{f'_{c-l}}{f'_{c-w}} = -a \cdot (\gamma_l - 72.8) + 1 \tag{3}$$

where,

a: experimental constant (m/N)

This means that the larger the value of a in Eq.3, the larger the influence of the surface tension of immersion

Table 3 Compressive strength of cement based materials immersed in various kinds of liquids with different surface tensions.

Types of cement based materials	W/C	Immersion liquid	Surface tension of immersion liquid (N/m)	Compressive strength of cement based materials (N/mm^2)
Cement paste(*) (Asamoto and Ishida 2004)	0.35	Ethanol	0.0220	55.0
		Oil	0.0271	50.1
		Water	0.0720	33.6
		No-liquid	-	71.0
	0.6	Ethanol	0.0220	40.6
		Oil	0.0271	43.4
		Water	0.0720	22.6
		No-liquid	-	49.7
Concrete(**) (Cook and Haque 1974)	0.4	Methanol	0.0221	54.2
		Water	0.0728	48.4
		No-liquid	0	64.5
Mortar(**) (Cook and Haque 1974)	0.3	Methanol	0.0221	66.3
		Water	0.0728	64.1
		No-liquid	0	85.5
	0.5	Methanol	0.0221	46.4
		Water	0.0728	38.6
		No-liquid	0	53.6

(*) Cylinders of φ50 × 100 mm were used. After underwater curing for 28 days, the specimens were dried in a drying furnace at 105 degrees C until the weight of the specimens was constant.
Then the specimens were submerged in each liquid until their weight were constant. The compression tests were then carried out.
(**) Cylinders of φ76 × 152 mm were used. After curing at 94 ± 3% R. H. and 22 ± 2 degrees C for 28 days, the specimens were dried at 112 ± 2 degrees C for 35 days. The specimens were then submerged in each liquid for 7 days.

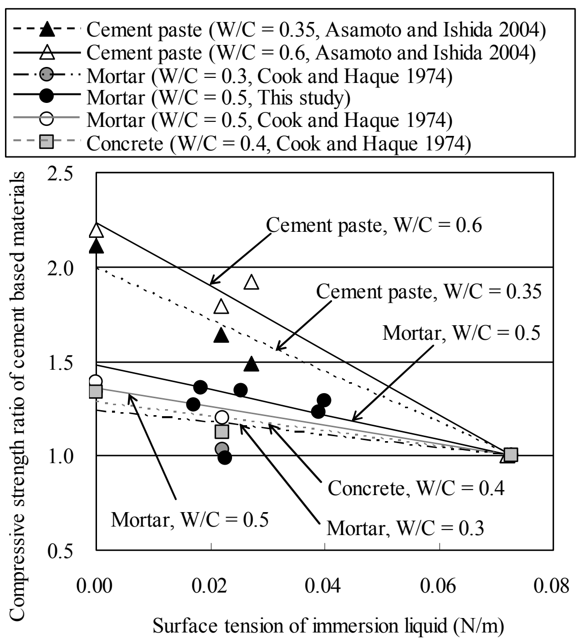

Fig. 5 Relationship between surface tension of immersion liquid and compressive strength ratio of cement based materials.

liquid on compressive strength. The values of a in Eq.3 are summarized in **Table 4**. The value of a for cement paste is the largest, followed by mortar, and it is the smallest for concrete. This order is considered to correspond to the volumetric cement paste content. This is because microcracks due to compression are generated mainly in the cement paste matrix except for high-strength concrete. When using the same type of cement based material, the higher the water-cement ratio, the larger the value of a. This is because the higher the water-cement ratio, the higher the void and liquid content of the cement based material.

From the observations mentioned above, it became clear that the compressive strength of cement based materials differs noticeably for different surface tensions of the immersion liquid. This indicates that the lower compressive strength of concrete in a wet condition is attributed to the lower surface energy that forms new microcracks through the surface tension of the water. It is also suggested that the compressive strength of concrete structures in contact with seawater or liquefied gas, such as marine structures and PCLNG tanks, differs from that of underwater structures.

Table 4 Value of a in Eq. 3.

Types of cement based materials	W/C	Volumetric cement paste content (m^3/m^3)	The value of a in Eq. 3
Cement paste (Asamoto and Ishida 2004)	0.35	1.00	13.6
	0.6	1.00	17.0
Mortar (Cook and Haque 1974)	0.3	0.69	3.3
	0.5	0.42	4.9
Mortar (This study)	0.5	0.46	6.6
Concrete (Cook and Haque 1974)	0.4	0.40	3.9

Table 5 Mixture of concrete used in the experiment.

W/C (%)	s/a*1 (%)	Unit quantity (kg/m^3)			
		Water	Cement	Sand	Gravel
55	47	165	300	846	1054

*1 : Volume ratio of sand to aggregate

Table 6 Surface tensions of liquids used in the experiment.

Name of liquid	Content	Surface Tension (N/m)
Liquid A	Air entraining agent solution diluted 20 times	0.0630
Liquid B	4 mol/l NaCl solution	0.0901

4. Influence of surface tension of immersion liquid on compressive fatigue strength of concrete

4.1 Methods and materials

Ordinary Portland cement (specific gravity = 3.16, specific surface = 0.327 m^2/g), sea sand (specific gravity in saturated surface-dry condition = 2.59, water absorption = 1.40%) and crushed stone (maximum size = 20 mm, specific gravity in saturated surface-dry condition = 2.86, water absorption = 1.19%) were used to make concrete specimens. An air-entraining and water-reducing agent (lignin sulfonic acid type) and an air-entraining agent (alkyl allyl sulfonic acid type) were also used. The concrete mixture used in the experiment is shown in **Table 5**. Trial mixing of concrete was done to achieve the target slump of 80 mm and the target air content of 4.5%.

Cylindrical specimens (ϕ75 × 150 mm) were used. Concrete was cast into a steel mold in 2 layers and rodding was applied six times to each layer. Then the outside of the mold was patted with a wooden hammer to fill the holes caused by the rodding, and finally the concrete was compacted on a vibrating table. Demolding was done 24 hours after casting and the specimens were cured in a room where the temperature was kept at 20 ± 1 degrees C and the relative humidity maintained higher than 90%.

As fatigue tests take a long time, the compressive strength of the concrete may change during such testing if it is performed while the hydration reaction of concrete is insufficient. Therefore, the concrete specimens used for the fatigue test were cured for more than 3 months.

In this study, two kinds of liquids with different surface tensions were used. In the previous chapter, organic solvents were used as liquids with different surface tensions. Fatigue tests, however, take a long time and using organic solvents may be dangerous owing to their high volatility. To preclude such risk, two liquids, an air entraining agent solution diluted 20 times (Liquid A) and a 4 mol/l NaCl solution (Liquid B) were used instead of organic solvent (**Table 6**). The surface tensions of both solutions are 0.0630 N/m and 0.0901 N/m, respectively. The NaCl solution was concocted by heating purified water to approx. 50 degrees C and then mixing in refined salt. The solution was well stirred, cooled to the room temperature and used for the experiments. No chloride crystals were observed in the solution after it was cooled.

Figure 6 shows the preparation procedure of the concrete specimens. First, the concrete specimens were mildly dried for 3 days in a temperature and relative humidity controlled room (temperature = 20 degrees C and relative humidity = 60%). Second, the specimens were dried in a drying furnace for 3 days at 60 degrees C and then for 7 days at 90 degrees C. Third, the specimens were removed from the drying furnace and cooled at room temperature. Finally, the specimens were submerged in each liquid for 14 days before the tests.

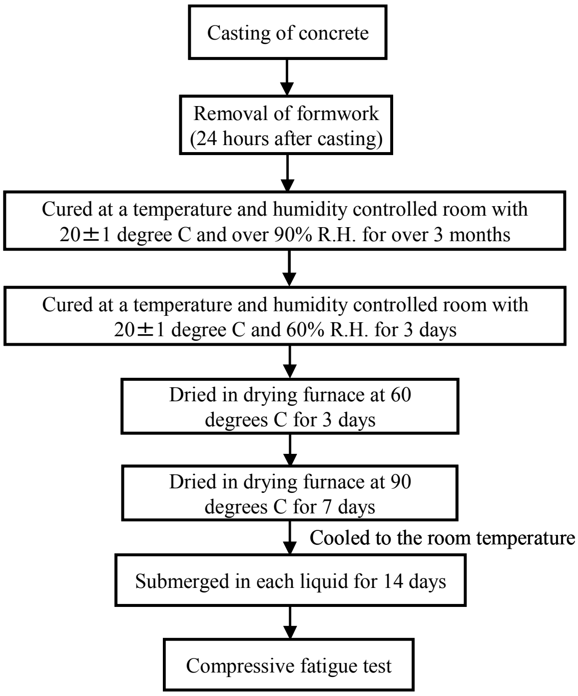

Fig. 6 Preparation procedure of concrete specimens.

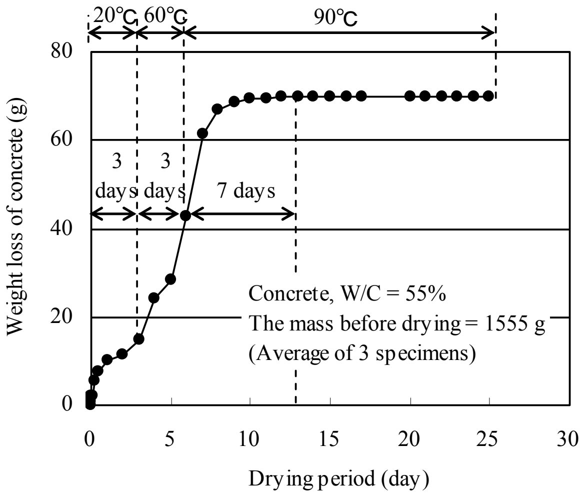

Fig. 7 Example of weight loss of concrete specimen when dried at 20, 60 and 90 degrees C after moisture curing for 91 days.

Figure 7 shows an example of the weight loss of concrete specimens when dried at 20, 60 and 90 degrees C after being moisture cured for 91 days. The plot shows that the total weight loss of the specimens converges to a constant value after they are dried at 90 degrees C for 7 days. At that point, concrete specimens are considered to reach their absolute dry condition.

Compressive strength was measured for each specimen group before and after the fatigue tests. The average of 5 values of the compressive strength obtained before the tests was adopted as the standard value of repeating stress ratios in the fatigue test. To investigate whether the compressive strength of concrete progressed or not, compressive strength was measured again after the fatigue test. Should the strength be found to increase, the stress ratios would be corrected.

The setting of the fatigue test is shown in **Fig. 8**. Each liquid was pooled in a container made of acrylic boards and a steel plate. Fatigue tests were performed with the concrete specimens submerged in liquid. An electrohydraulic servo fatigue test machine (load capacity = 200 kN) was used. As the wave shape of loading, a sinusoidal waveform was employed. First, the loading frequency was 1 Hz until the loading cycle number reached 100 cycles. Then the loading frequency was increased gradually to 5 Hz until the loading cycle number reached 200 cycles. The lower limit of the stress applied to the specimens was 10% of their compressive strengths. The upper limits were 55, 60, 65, 70 and 75% of the compressive strength when liquid A was used, and 45, 50, 55, 60 and 65% of the compressive strength when liquid B was used. The maximum stress ratio S_{max} and the minimum stress ratio S_{min} are given by Eq.4 and Eq.5, respectively.

$$S_{\max} = \sigma'_{\max} / f'_{c-l} \tag{4}$$

$$S_{\min} = \sigma'_{\min} / f'_{c-l} \tag{5}$$

where σ'_{max} is the maximum stress, σ'_{min} is the minimum stress, and f'_{c-l} is the compressive strength of concrete in each liquid.

For each stress ratio, 5 specimens were tested. The fatigue test was terminated when the specimen fractured or the loading cycle number reached 2×10^6 cycles.

4.2 Experimental results

4.2.1 Static strength of concrete under static compressive stress in liquids having different surface tensions

Table 7 summarizes the results of the compressive strength tests. For comparison, the test results in water are also listed. There being little difference in the compressive strengths before and after the fatigue test, av-

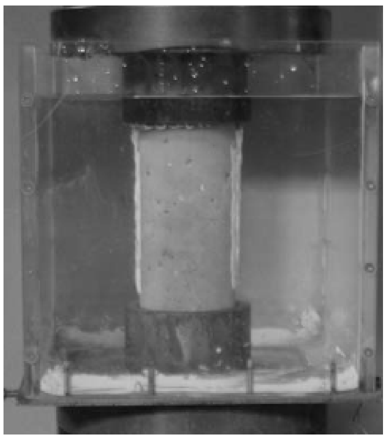

Fig. 8 Setting of compressive fatigue test.

Table 7 Results of compressive strength test of concrete in liquids.

Test environment	Timing of Compressive Strength measurement	Specimen No.	Compressive strength of concrete (N/mm^2)	Average value (N/mm^2)	Standard Deviation (N/mm^2)	Coefficient of variance (%)
In water (Surface tension = 0.0728 N/m)	-	No. 1	31.8	31.7	1.5	4.6
		No. 2	29.4			
		No. 3	32.5			
		No. 4	31.6			
		No. 5	33.4			
In liquid A (Surface tension = 0.0630 N/m)	Before Fatigue test	No. 1	31.7	32.1	1.3	3.9
		No. 2	31.4			
		No. 3	30.6			
		No. 4	34.7			
	After Fatigue test	No. 5	32.8			
		No. 6	31.2			
		No. 7	33.4			
		No. 8	32.7			
		No. 9	31.2			
		No. 10	31.6			
In liquid B (Surface tension = 0.0901 N/m)	Before Fatigue test	No. 1	28.4	29.2	1.0	3.5
		No. 2	28.9			
		No. 3	29.7			
		No. 4	27.3			
		No. 5	29.8			
	After Fatigue test	No. 6	30.1			
		No. 7	29.6			
		No. 8	28.3			
		No. 9	30.9			
		No. 10	29.2			

erage values, standard deviations and coefficients of variation of the compressive strength were calculated from a total of 10 data.

Figure 9 shows the relationship between the surface tension of the immersion liquid and the compressive strength of concrete. It is recognized that the bigger the surface tension of the immersion liquid, the smaller the compressive strength of concrete. This is because the surface energy that forms new microcracks decreases as the surface tension of the immersion liquid increases. In the previous chapter, it became clear that there is a linear relationship between the surface tension of the immersion liquid and the compressive strength of concrete. The regression equation between the surface tension of the immersion liquid and the compressive strength of concrete is given by Eq.6.

$$f'_{c-l} = -111\gamma_l + 39.4 \tag{6}$$

As this expression is an empirical equation obtained from a limited experimental data, the range of its application is limited when the surface tension of immersion liquid is between 0.0630 N/m to 0.0901 N/m. Further, in the case of different components or material age, Eq.6 cannot be applied without modifications.

In Chapter 3, it was experimentally confirmed that there is a linear relationship between the surface tension of the immersion liquid and the compressive strength of the mortar, including the case when the internal void of the mortar is saturated with no liquid (i.e. the surface tension = 0 N/m). Thus, there is the possibility that Eq.6 is effective when the surface tension of the liquid is 0 N/m. In Eq.6, by setting γ_l to 0 N/m, we can obtain the value of the compressive strength of concrete in air, 39.4 N/mm^2. We can also obtain the value of the compressive strength of the concrete in water by setting γ_l to 0.0728 N/m, 31.3 N/mm^2. Therefore, under the conditions of this study, the compressive strength of the concrete in water is 26% smaller than that in air.

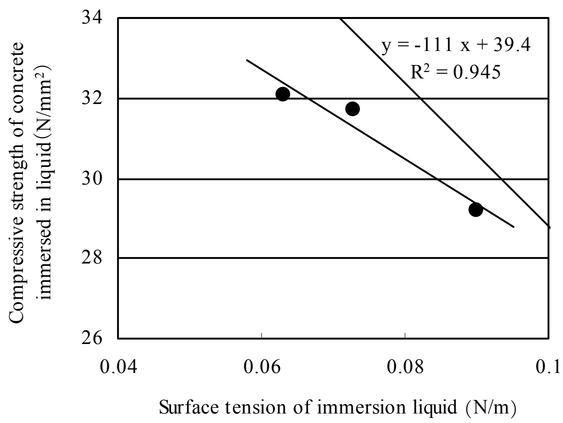

Fig. 9 Relationship between surface tension of immersion liquid and compressive strength of concrete.

As mentioned above, it was reconfirmed that the compressive strength of concrete decreases linearly with increases in the surface tension of the immersion liquid.

4.2.2 Fatigue strength of concrete under cyclic compressive stress in liquids having different surface tensions

Generally, the fatigue test results are widely spread, making a statistical method indispensable for their analysis. Moreover, if the number of specimens is small as in this study, it is necessary to consider the survival probability (Matsushita and Tokumitsu 1979) and apply the theory of order statistics (Gumbel 1958). The survival probability expectation, $P(N_r)$, of a specimen that has the rth smallest fatigue life out of a total of n specimens is given by Eq.7.

$$P(N_r) = 1 - \frac{r}{n+1} \quad (7)$$

Equation 7 can be used when all specimens in one group are fractured by the specified cycle number of N_X. Usually, the value of N_X is 2×10^6. If not all the specimens are fractured by the cycle number of N_X, another procedure is employed. When m specimens out of a total of n are not fractured by the cycle number of N_X, it is assumed that a total of (n+1) specimens were tested and a specimen with (n–m+1)th smallest fatigue life is fractured at the cycle number of N_X. Then the survival probability expectation, $P(N_r)$, of the specimen with the rth smallest fatigue life and of the specimen that is fractured at the cycle number of N_X are given by Eq.8 and Eq.9, respectively (Hamada *et al.* 1971).

$$P(N_r) = 1 - \frac{r}{n+2} \quad (8)$$

$$P(N_r) = 1 - \frac{n-m+1}{n+2} \quad (9)$$

The value of the fatigue life and $P(N_r)$ obtained in this study are shown in **Table 8**. Since the fatigue life of concrete is logarithmically distributed (Matsushita and Tokumitsu 1979), the data obtained in this study are plotted on a lognormal probability graph. **Figure 10** shows the *P-N* diagrams, where each test result set is well approximated by a straight line. However, in the case of the maximum stress ratio of 45% using liquid B, neither of the 3 specimens were fractured by the cycle number of 2×10^6, so the data is not approximated by a straight line.

When fatigue life is logarithmically distributed, the regression equation is given by Eq.10.

$$t = A \log N + B \quad (10)$$

where,

t: the distance of a point on a normal distribution curve from an axis of symmetry determined from a normal integral table by using the value of $P(N_r)$

A, B: experimental constants.

Table 8 Measured fatigue life and $P(N_r)$.

Test environment	σ'_{max} / f'_{c-l} (%)	r	Fatigue life (cycles)	$\log N_r$	$P(N_r)$
In liquid A	75	1	2422	3.38	83.3
		2	3796	3.58	66.7
		3	5550	3.74	50.0
		4	7813	3.89	33.3
		5	9110	3.96	16.7
	70	1	20041	4.30	83.3
		2	22545	4.35	66.7
		3	30593	4.49	50.0
		4	35402	4.55	33.3
		5	44442	4.65	16.7
	65	1	41083	4.61	83.3
		2	52679	4.72	66.7
		3	82196	4.91	50.0
		4	172214	5.24	33.3
		5	318536	5.50	16.7
	60	1	61917	4.79	83.3
		2	201213	5.30	66.7
		3	525042	5.72	50.0
		4	627433	5.80	33.3
		5	835498	5.92	16.7
	55	1	393204	5.59	85.7
		2	653554	5.82	71.4
		3	1232407	6.09	57.1
		4	1834670	6.26	42.9
		5	2000000→		
In liquid B	65	1	9801	3.99	83.3
		2	21964	4.34	66.7
		3	24674	4.39	50.0
		4	32624	4.51	33.3
		5	33218	4.52	16.7
	60	1	29950	4.48	83.3
		2	57556	4.76	66.7
		3	69485	4.84	50.0
		4	97296	4.99	33.3
		5	110731	5.04	16.7
	55	1	133938	5.13	83.3
		2	163529	5.21	66.7
		3	224669	5.35	50.0
		4	248553	5.40	33.3
		5	291952	5.47	16.7
	50	1	374388	5.57	83.3
		2	400611	5.60	66.7
		3	518903	5.72	50.0
		4	661840	5.82	33.3
		5	817267	5.91	16.7
	45	1	2000000→		
		2	2000000→		
		3	2000000→		

The average fatigue life, $\overline{\log N}$, and the standard deviation, $D(\log N)$, are calculated with Eq.11 and Eq.12.

$$\overline{\log N} = -\frac{B}{A} \tag{11}$$

$$D(\log N) = \frac{1}{|A|} \tag{12}$$

The expressions of the linear regression equations, the values of the multiple correlation coefficients, $\overline{\log N}$ and $D(\log N)$ are shown in **Table 9**. From the values of multiple correlation coefficients, it is confirmed that the fatigue life fits well a straight line. The values of $D(\log N)$ are 0.19-0.58 for liquid A, and 0.18-0.29 for liquid B. There is a tendency for the value of $D(\log N)$ to be smaller the bigger the surface tension of the immersion liquid. Matsushita (1980) reported that the fatigue life spread of concrete in water is remarkably smaller than that of concrete in air and stated that whereas internal voids in concrete are completely filled with water in an in-water fatigue test, in an in-air fatigue test, internal voids of concrete are partially filled with water and there is little difference between specimens. Further, due to differences in relative humidity during testing, the air that filled the internal voids of concrete had a different relative humidity depending on the time when the tests were performed. In previous works, the values of $D(\log N)$ were 0.8-1.5 in in-air fatigue test (Matsushita and Tokumitsu 1979) and 0.5-1.0 in in-water fatigue test (Matsushita 1980).

Figure 11 shows the *S-N* curves for concrete specimens immersed in various kinds of liquids. The standard values of stress ratios are static strengths measured in each liquid (f'_{c-l}). For comparison, the regression lines obtained in the previous works (Matsushita and Tokumitsu 1979; Matsushita 1980) are also shown in the figure. There is a linear relationship between σ'_{max}/f'_{c-l} and $\overline{\log N}$. Compared with the same average fatigue life, $\overline{\log N}$, the bigger the surface tension of immersion liquid, the smaller the fatigue strength, σ'_{max}/f'_{c-l}. This is because the progression of the microcracks is accelerated by decreases in the surface energy released on new microcracks under the influence of the liquid surface tension. Arthur *et al.* (1979) investigated the fatigue properties of RC beams in seawater and reported that the fatigue life of RC beams decreases considerably compared to that in air. This is in agreement with the results of this study.

4.2.3 *S-N* curve considering minimum stress ratio

The relationship between maximum stress ratio and average fatigue life, or the *S-N* curve, differs for different minimum stress ratios. When the maximum stress ratio is constant, the larger the minimum stress ratio, the longer the fatigue life of concrete. According to a previous study (Matsushita and Tokumitsu 1979), the time-endurance curve, which expresses the relationship between the minimum stress ratio and the limit value of the maximum stress ratio at which concrete does not fracture due to fatigue caused by cycle number N, can be approximated by a straight line that passes through the point (S_{min}, S_{max}) = (100%, 100%). It is also known that the modified Goodman relationship is applicable when the minimum stress ratio is under 60% of the static strength of concrete.

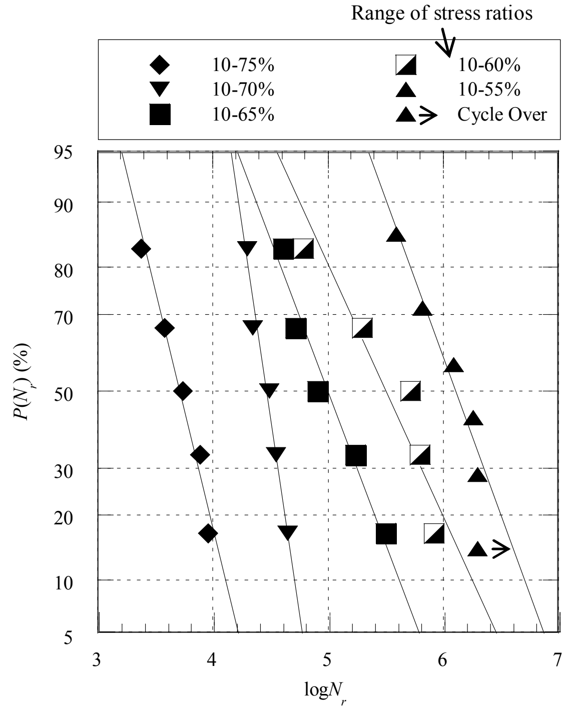

Fig. 10 (a) *P-N* diagram (measured in liquid A).

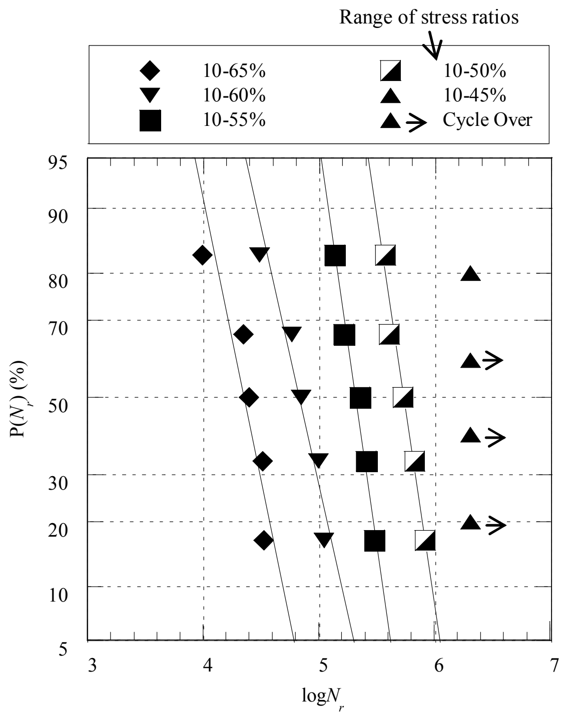

Fig. 10 (b) *P-N* diagram (measured in liquid B).

Table 9 Linear regression equations, multiple correlation coefficients, log*N* and *D*(log*N*).

Test environment	σ'_{max}/f'_{c-l} (%)	Linear regression equation	Multiple correlation coefficient (R^2)	$\overline{\log N}$	*D* (log*N*)
In liquid A	75	$t = -3.247\log N_r + 12.05$	0.969	3.712	0.31
	70	$t = -5.376\log N_r + 24.02$	0.978	4.467	0.19
	65	$t = -2.079\log N_r + 10.39$	0.961	4.998	0.48
	60	$t = -1.721\log N_r + 9.48$	0.890	5.507	0.58
	55	$t = -2.160\log N_r + 13.20$	0.957	6.112	0.46
In liquid B	65	$t = -3.831\log N_r + 16.67$	0.823	4.352	0.26
	60	$t = -3.472\log N_r + 16.74$	0.932	4.822	0.29
	55	$t = -5.525\log N_r + 29.34$	0.966	5.311	0.18
	50	$t = -5.319\log N_r + 30.45$	0.964	5.725	0.19

In such cases, the relationship between the repeating stress ratios and average fatigue life is given by Eq.13.

$$\overline{\log N} = K_1 \frac{f'_{c-l} - \sigma'_{max}}{f'_{c-l} - \sigma'_{min}} + K_2 \quad (13)$$

where K_1 and K_2 are experimental constants that are independent of the repeating stress ratios and the fatigue life of concrete. In general, K_2 is almost zero and can be neglected. Thus, Eq.14 is proposed as a more concise equation.

$$\overline{\log N} = K \frac{f'_{c-l} - \sigma'_{max}}{f'_{c-l} - \sigma'_{min}} \quad (14)$$

where *K* is an experimental constant with different values depending on the moisture content or type of concrete.

Figure 12 shows the relationship between $\overline{\log N}$ and $(f'_{c-l} - \sigma'_{max}) / (f'_{c-l} - \sigma'_{min})$. For comparison, the regression lines reported in the previous works (Matsushita and Tokumitsu 1979; Matsushita 1980) are also plotted. The *S-N* curve equations considering minimum stress ratios are listed in **Table 10**. The values of *K* are in the following order from highest to smallest, in air, in liquid A, in water and in liquid B. That is to say, the larger the surface tension of the immersion liquid, the smaller the *K* value.

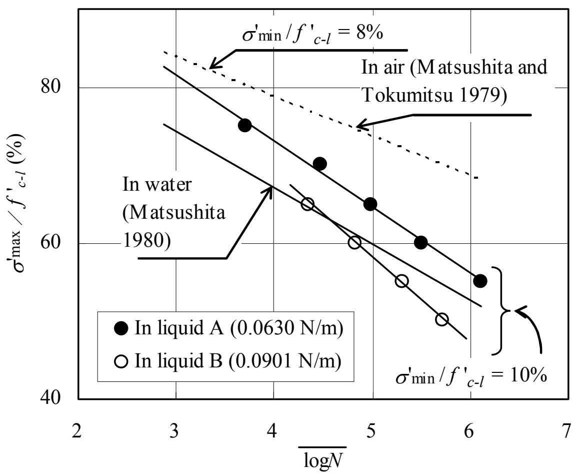

Fig. 11 *S-N* curves of this study and previous works.

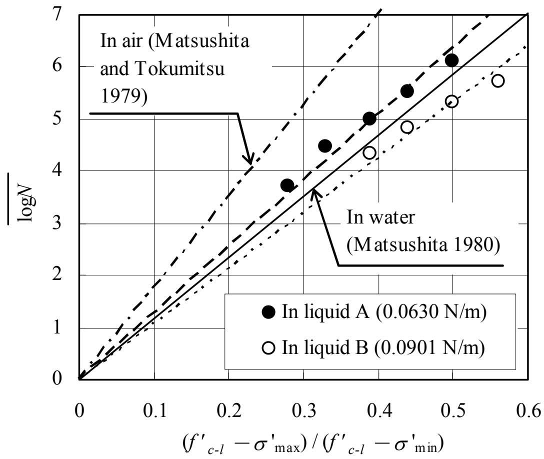

Fig. 12 *S-N* curves considering minimum stress ratio.

Table 10 *S-N* curve equations considering minimum stress ratios.

Test environment	*S-N* curve equation considering minimum stress ratio	Multiple Correlation Coefficients (R^2)
In liquid A	$\log N = 12.7 \frac{f'_{c-l} - \sigma'_{max}}{f'_{c-l} - \sigma'_{min}}$	0.952
In liquid B	$\log N = 10.6 \frac{f'_{c-l} - \sigma'_{max}}{f'_{c-l} - \sigma'_{min}}$	0.893
In air	$\log N = 17.5 \frac{f'_{c-l} - \sigma'_{max}}{f'_{c-l} - \sigma'_{min}}$	-
In water	$\log N = 11.7 \frac{f'_{c-l} - \sigma'_{max}}{f'_{c-l} - \sigma'_{min}}$	-

Figure 13 shows the relationship between the surface tension of the immersion liquid and the *K* value. It is recognized that the *K* value decreases linearly as the surface tension of the immersion liquid increases. This is because the bigger the surface tensions of the immersion liquid, the smaller the surface energy that forms new microcracks in concrete by loading. As a result, the fatigue life of concrete decreases with increases in the surface tension of the immersion liquid.

The relationship between the surface tension of the immersion liquid, γ_l, and the *K* value obtained from this study and previous works is given by Eq.15.

$$K = -77.0\gamma_l + 17.5 \tag{15}$$

That is to say, *K* decreases 77.0 per 1 N/m increase in the surface tension of the immersion liquid.

As discussed above, it became clear that the fatigue life of concrete in various liquids with different surface tensions is logarithmically distributed, and the *K* value in the Goodman-type *S-N* curve equation (Eq.14) decreases linearly with increases in the surface tension of the immersion liquid.

4.3 A discussion about the standard value of repeating stress ratios

Generally, in fatigue tests, the value of the static strength of concrete with the same components and moisture content is used as the standard value of the repeating stress ratio. On the other hand, the static strength of concrete differs greatly for different surface tensions of the immersion liquid. This poses the problem that the fatigue strengths of concrete with different moisture contents cannot be easily compared.

According to the standard specifications for concrete structures (JSCE 2002), the design strength of concrete is essentially determined based on the strength at the material age of 28 days. It is also stated that the design strength can be determined by the strength at a proper material age corresponding to the timing when major loading begins to be applied to the structure.

Ordinarily, the compressive static strength of concrete in a wet condition is used as the design strength. Therefore, the value of fatigue strength with setting of the static strength of concrete in a wet condition as the standard value of repeating stress ratios was investigated.

By transforming Eq.14, Eq.16 is obtained.

$$\frac{\sigma'_{max}}{f'_{c-l}} = 1 - \frac{\log N}{K}\left(1 - \frac{\sigma'_{min}}{f'_{c-l}}\right) \tag{16}$$

The static strength of concrete in the completely wet condition is set as f'_{c-w}. By multiplying both sides of Eq.16 by f'_{c-l} / f'_{c-w}, the *S-N* curve equation with setting of the static strength of concrete in the completely wet condition as the standard value of repeating stress ratios (Eq.17) is obtained.

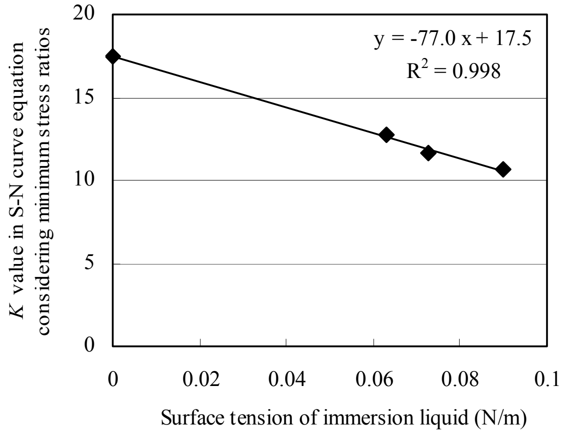

Fig. 13 Relationship between surface tension of immersion liquid and *K* value in Goodman type *S-N* curve equation.

$$\frac{\sigma'_{max}}{f'_{c-w}} = \frac{f'_{c-l}}{f'_{c-w}}\left\{1 - \frac{\log N}{K}\left(1 - \frac{\sigma'_{min}}{f'_{c-l}}\right)\right\} \tag{17}$$

Next, several immersion liquids with different surface tensions are considered; (1) 0 N/m, (2) 0.0400 N/m, (3) 0.0728 N/m and (4) 0.0900 N/m. Liquids (1), (3) and (4) are assumed as air, water and concentrated seawater, respectively. Using Eq.6, the static strength of concrete in liquid, f'_{c-l}, is obtained. The *K* value in the Goodman-type *S-N* curve equation is obtained by using Eq.15. **Table 11** summarizes the calculation results. By substituting these values into Eq.16 and Eq.17, the following discussion is processed.

First, we considered the case of a complete pulsating loading in which the minimum stress ratio, σ'_{min}/f'_{c-l}, is equal to 0%. When the static strength of concrete in each liquid, f'_{c-l}, is set as the standard value of repeating stress ratios, the *S-N* curves is plotted as shown in **Fig. 14 (Case A)** by using Eq.16. On the other hand, if the static strength of concrete in the completely wet condition, f'_{c-w}, is set as the standard value of the repeating stress ratios, the *S-N* curves can be plotted as shown in **Fig. 14 (Case B)** by using Eq.17. The static strength of concrete in the

Table 11 Value of f_{c-l} and *K* calculated from Eq. 5 and Eq. 13.

Test environ-ment	Surface tension of immersion liquid (N/m)	f'_{c-l} calculated from Eq. 6 (N/mm²)	*K* calculated from Eq. 15
①	0	39.4	17.5
②	0.0400	35.0	14.4
③	0.0728	31.3	11.9
④	0.0900	29.4	10.6

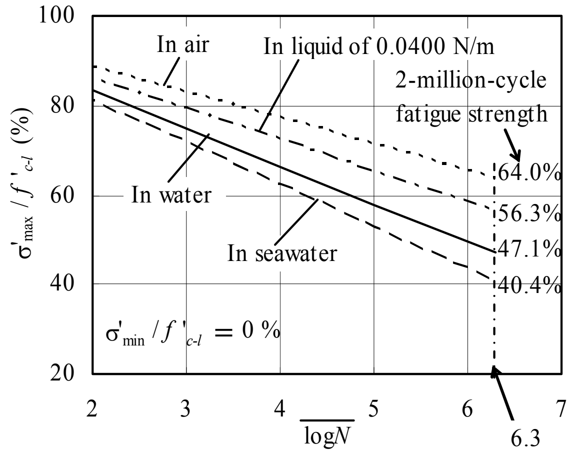

Fig. 14 (a) *S-N* curve with setting $f'_{c\text{-}l}$ as standard values of stress ratios (minimum stress ratio = 0%).

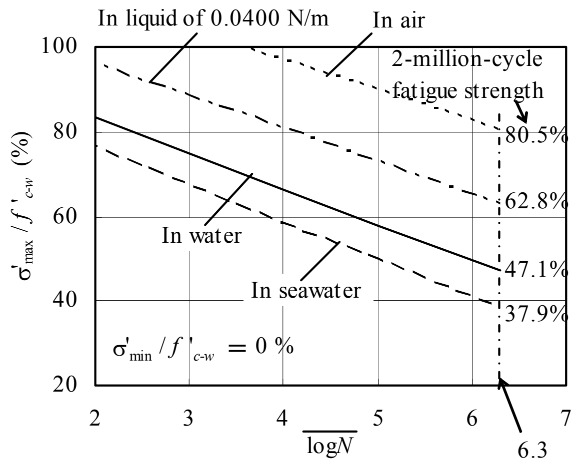

Fig. 14 (b) *S-N* curve with setting $f'_{c\text{-}w}$ as standard values of stress ratios (minimum stress ratio = 0%).

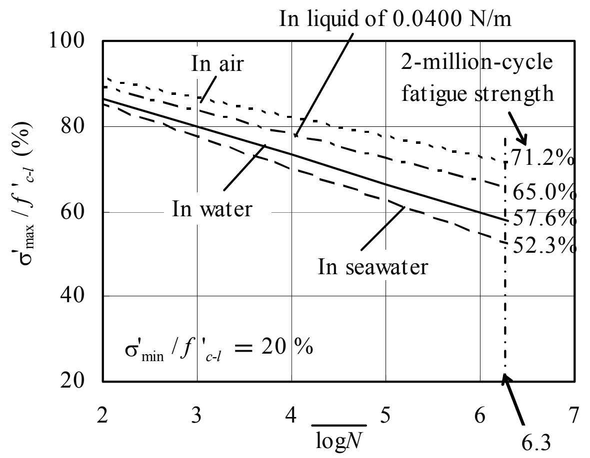

Fig. 15 (a) *S-N* curve with setting $f'_{c\text{-}l}$ as standard values of stress ratios (minimum stress ratio = 20%).

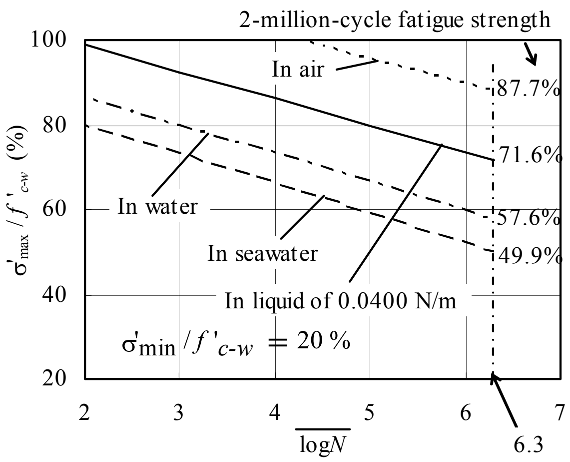

Fig. 15 (b) *S-N* curve with setting $f'_{c\text{-}w}$ as standard values of stress ratios (minimum stress ratio = 20%).

completely wet condition is known not to differ much from that of concrete in water (Matsushita 1980). Therefore, in this study, $f'_{c\text{-}w}$ is substituted with the static strength of concrete in water. The 2-million-cycle fatigue strengths of concrete in each liquid are (1) 80.5%, (2) 62.8%, (3) 47.1% and (4) 37.9%, respectively. That is to say, in the case of complete pulsating loading, the fatigue strength of concrete in water is 33.4% smaller than that of concrete in air. On the other hand, the static strength of concrete in water was 26% smaller than that in air, as mentioned in 4.2 (1). The difference in the fatigue strengths of concrete is larger than the difference of the static strengths of concrete. This is because the amount of microcracks generated in concrete under repeated loading is greater than that of static loading.

Secondly, assuming a dead load of structures, the minimum stress ratio, $\sigma'_{\min}/f'_{c\text{-}l}$, is set to 20%. In that case, the *S-N* curves with setting of the static strength of concrete in each liquid, $f'_{c\text{-}l}$, as the standard value of repeating stress ratios are plotted in **Fig. 15 (Case A)**. The plots of the *S-N* curves with setting of the static strength of concrete in water, $f'_{c\text{-}w}$, as the standard value of repeating stress ratios, are shown in **Fig. 15 (Case B)**. The 2-million-cycle fatigue strengths of concrete in each liquid are (1) 87.7%, (2) 71.6%, (3) 57.6% and (4) 49.9%, respectively. In this case, the fatigue strength of concrete in water is 32% smaller than that in air.

Compared with **Fig. 14 (Case A)** and **Fig. 15 (Case A)**, in **Fig. 14 (Case B)** and **Fig. 15 (Case B)**, the difference of fatigue strength due to the surface tension of the immersion liquid is significantly large. In particular, the fatigue strength increases significantly when the specimen is immersed in liquid with a smaller surface tension than water. This means that the fatigue strength of concrete in air hardly matters. On the other hand, the fatigue strength of concrete immersed in liquid with a larger surface tension than water is much smaller than that in water. This fact indicates that special attention to fatigue loading in the design of concrete members should be given when concrete structures are frequently immersed in liquid with a larger surface tension than water, such as marine structures.

5. Conclusions

An experimental study was conducted to investigate the effect of the surface tension of the immersion liquid on the compressive static and fatigue strength of concrete. The following conclusions were obtained:

(1) The compressive static strength of cement based materials decreases linearly with increases in the surface tension of the immersion liquid.

(2) The lowering of the compressive strength of concrete in a wet condition can be explained as the decrease in the surface energy that forms new microcracks.

(3) The influence of the surface tension of the immersion liquid on the compressive strength is different for different types of cement based materials.

(4) The larger the water-cement ratio, the larger the influence of the surface tension of the immersion liquid on the compressive strength.

(5) The fatigue life of concrete in liquid with a different surface tension than water is logarithmically distributed.

(6) The K value in the Goodman-type S-N curve equation (Eq.14) decreases linearly with increases in the surface tension of the immersion liquid. From the regression equation obtained in this study (Eq.15), the K value decreases 77.0 per 1 N/m increase in the surface tension of the immersion liquid.

(7) Special attention to fatigue loading should be given when concrete structures are frequently immersed in liquid with a larger surface tension than water, such as marine structures.

Acknowledgements

The authors would like to extend their appreciation to former Kyushu University students Mr. M. Hashimoto, Mr. M. Wakabayashi and Mr. H. Onishi for their efforts in carrying out this study. Moreover, the measurements of the surface tensions of the liquids were made using the surface tension measurement equipment at the Center of Advanced Instrumental Analysis, Kyushu University.

References

Asamoto, S. and Ishida, T. (2004). "Microscopic approach to time-dependent deformation mechanism of concrete based on liquid characteristics." *Journal of Materials*, *Concrete Structures*, *Pavements*, *JSCE*, 50(760), 159-172.

Cook, D. J. and Haque, M. N. (1974). "Strength reduction and length changes in concrete and mortar on water and methanol sorption." *Cement and Concrete Research*, 4(5), 735-744.

Griffith, A. A. (1920). *Phil. Trans. Roy. Soc.*, 221, 163.

Gumbel, E. J.(1958). "Statistics of extremes." *Columbia University Press*,

Hori, M. (1962). "The strength of cement based materials from the viewpoint of surface energy." *Journal of the Ceramic Association, Japan*, 70(7), 54-59.

Matsushita, H. and Tokumitsu, Y. (1979). "A study on compressive fatigue strength of concrete considered survival probability." *Journal of Materials*, *Concrete Structures*, *Pavements*, *JSCE*, 284, 127-138.

Matsushita, H. (1980). "A study on compressive fatigue strength of concrete in the water." *Journal of Materials*, *Concrete Structures*, *Pavements*, *JSCE*, 296, 87-95.

Ogishi, S., Ono, H. and Tanahashi, I. (1986). "Influence of surface tension of several kinds of impregnated liquids on the strength and Young's modulus of cement mortar." *Fracture Toughness and Fracture Energy of Concrete*, *Elsevier Science Publishers*, *Amsterdam*, 215-218

Okajima, T. and Ishikawa, T. (1981). "Moisture content dependency of the strength of cement based materials from the viewpoint of surface energy." *Annual Report on the Cement Technology*, 35, 130-133.

Oshita, H. and Taniguchi, Y. (1999). "Experimental and analytical study on fracture energy of concrete as a porous permeable material partially saturated with water." *Journal of Materials*, *Concrete Structures*, *Pavements*, *JSCE*, 43(620), 257-270.

Pickett, G. (1956). "Effect of aggregate on shrinkage of concrete and a hypothesis concerning shrinkage." *Journal of ACI*, 52(1), 581-590

Troxell, G. E. (1958). "Long-time creep and shrinkage tests of plain and reinforced concrete." *Proceedings of ASTM*, 58, 1101-1120.

Wittmann, F. H. (1983). "Structure of concrete with respect to crack formation." *Fracture Mechanics of Concrete*, *F. H. Wittmann editor*, *Elsevier Science Publishers*, 43-74